GRAPHENE NANOCOMPOSITES AS STRAIN-DAMAGE SENSOR

M. Sanchez*, R. Moriche, S.G. Prolongo, J. Rams, A. Ureña

Dpt. Materials Science and Engineering, University Rey Juan Carlos, C/Tulipán s/n, Móstoles, 28933, Madrid, Spain

* maria.sanchez@urjc.es

Keywords: Graphene, nanocomposite, smart material, strain sensor.

Abstract

Graphene filled epoxy composite can be used as strain sensor. By using sonication and calendaring processes, graphene nanoplatelets were dispersed into the matrix to fabricate the composite. The piezoresistive mechanism of the sensors with two different thickness nanoplatelets was studied analyzing the changes in the graphene network under tensile and flexural tests. The low effective content and the tendency to keep flat after dispersion of high thickness nanoparticles gave rise to sensors with high gauge factor.

1. Introduction

Carbon-based nanomaterials, especially carbon nanotubes (CNT) [1] and graphene [2], have gathered exceptional interest during the last decade due to their extraordinary mechanical, electrical and thermal properties, high surface area, chemical sensitivity, flexibility, transparency, etc. These carbon allotropes can be used in a wide range of smart materials developed for practical applications in advanced aerospace, mechanical parts, energy technology, bionics and medical technologies. There is also an interest in the structural health monitoring (SHM), and strain sensing using polymer nanocomposites have received much attention because the conductive networks formed in the polymer seems to be very sensitive to strain or damage, even at low loads. Theoretical and experimental research has been carried out on strain sensing behavior of CNT-polymer [3-6] and graphene–polymer [7-9] composites.

2. Experimental

2.1. Materials

The fabrication of GNP/epoxy nanocomposites was made with an epoxy resin obtained from a basic DGBA monomer (Araldite LY556) cured with an aromatic amine (Araldite XB3473). Two types of GNPs provided by *XGScience* were used: i) GNPs powder grade M, with an average thickness in the range of 6 nm and an average lateral size of 25 μm, and ii) GNPs powder grade H with an average thickness in the range of 15 nm and an average lateral size of 25 μm. The electrical conductivity data supplied by the manufacturer are similar for both GNPs, 10^7 S/m parallel to the surface and 10^2 in the perpendicular direction.

2.2. GNP/epoxy nanocomposites fabrication

Nanocomposites with GNP content of 3 wt. % using powders with grades M and H were manufactured. GNPs were dispersed in the monomer by 1) sonication followed by 2) calendaring which consisted in three steps. The conditions used in both processes are collected in Table 1. Afterwards, the GNP/epoxy mixtures were degassed under vacuum at 80 °C for 15 minutes to remove dissolved gas. Finally, the hardener was added in a weight ratio 100:23 (monomer: hardener) and the mixture was cured at 140 °C for 8 hours. To identify the samples the following code was used: Resin (LY), wt. % and type of GNPs.

Process	1- Sonication			2- Calendaring		
	Amplitude (%)	Cycle (s)	Time (min)	Repetitions	Rollers gap (μm)	Velocity (rpm)
1	50	0.5	45	-	-	-
2-1	-	-	-	1	5 - 5	250
2-2	-	-	-	1	5 - 5	300
2-3	-	-	-	1	5 - 5	350

Table 1. Conditions used in sonication and calendaring processes for dispersion of GNPs in the epoxy resin.

2.3. GNP/epoxy nanocomposites characterization

Electrical conductivity of nanocomposites doped with different types of GNPs was measured. DC volume conductivity was evaluated according to ASTM D257 using Source Meter Unit instrument (KEITHLEY 2410). Three samples (10 × 10 × 1 mm^3) were measured per each nanocomposite and the applied voltage was within the range of 0-10 V. The dispersion of nanoreinforcements in the matrix was evaluated from the analysis of the fracture surfaces of flexural tests by Scanning Electron Microscopy (*Hitachi 3400*).

2.4. Structural health monitoring tests

For the SHM measurement, silver electrodes were placed in samples using different configurations depending on the applied mechanical test (tensile or flexural), as shown in Figure 1. In tensile test, electrodes were placed forming a Cu contact ring at a distance of 30 mm (Figure 1a) in samples with dimensions according to the ASTM D638 with a thickness of 4 mm. Configurations under flexural test are plotted in Figures 1b and 1c in a sample with dimensions 60 × 12.7 × 1.7 mm^3 following ASTM D790. In the first one, contacts were placed in the lower side between the two cylinders with a separation of 12 mm (Figure 1b), where the material is mainly subjected to tensile loads. The second configuration used in flexural test consisted in locating the electrodes in the top side, where only one flexural cylinder is placed, maintaining the same distance of 12 mm, and in this zone compression loads prevail (Figure 1c).

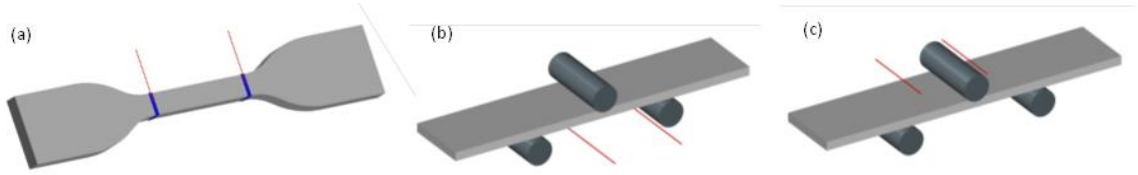

Figure 1. Contact configurations used in tensile (a) and (b,c) flexural tests.

Tensile and flexural tests were performed in a MTS Alliance RF/100 synchronized with the electrical measurements. For each configuration, electrical resistance was evaluated and recorded by an Agilent 34410A. The initial resistance between contacts was measured and its change was recorded by using the following equation:

$$R_N = \frac{R - R_0}{R_0} \quad (1)$$

where R is the measured electrical resistance at an instant and R_o is the initial electrical resistance of the nanocomposite for the chosen contact configuration. The corresponding sensitivity (gauge factor) of the samples was calculated as the relationship between the resistance variation (R_N) and strain (ε) according to the following expression:

$$S = \frac{R_N}{\varepsilon} \quad (2)$$

3. Results and discussion

3.1. Structural characterization of base materials and GNP/epoxy nanocomposites

The morphology of the as-received GNP powders was studied by SEM (Figure 2). The lateral size of both powders varied from 10 to 100 μm. At higher magnification it is possible to observe that H25 GNPs were more stacked (Figure 2b) than M25 ones (Figure 2a). The only difference indicated by the manufacturer was the higher number of graphene layers of the H25 particles. As the number of graphene layers of GNPs increases: i) the effective number of graphene nanoplatelets incorporated in the matrix and ii) the folding ability decrease. This last effect could give rise to higher van der Waals forces which keep H25 particles together.

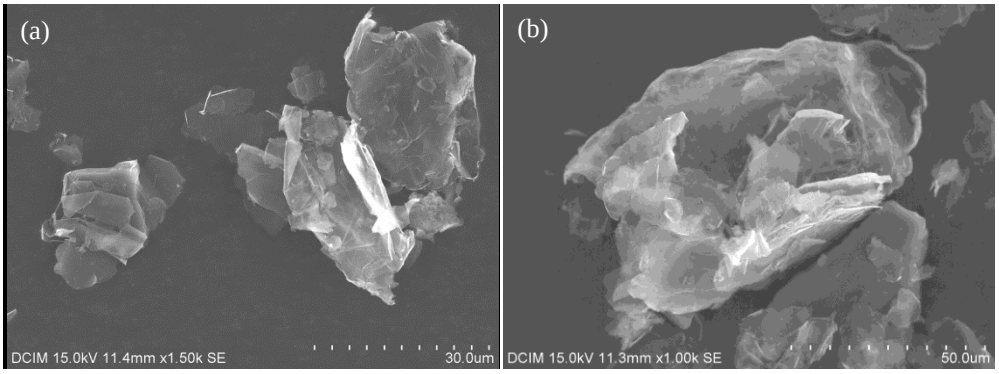

Figure 2. SEM images of as-received GNP powders grade (a) M and (b) H.

The electrical conductivity of nanocomposites is listed in Table 2. The conductivity of materials doped with M25 GNPs is lower than those reinforced with H25 ones. Conductivity in carbon based nanomaterials can be due to two mechanisms: 1) contact between conductive particles and 2) electron tunneling between them. In the last mechanism, the interparticle separation is in the order of nanometers. To explain the conductivity values, the morphology and the effective number of the nanoparticles in the matrix have to be also taken into account.

Nanocomposite	N. graphene layers of GNPs	σ (S/m)
LY3M25	6	$(3.7 \pm 0.7) \cdot 10^{-4}$
LY3H25	15	$(1.1 \pm 0.6) \cdot 10^{-3}$

Table 2. Electrical conductivity values of nanocomposites.

From the analysis of the fracture surfaces of flexural tests (Figure 3), that were made for the evaluation of structural heath monitoring capability of the nanocomposites and whose results will be explained in next section, the effective number of nanoparticles and their morphology can be established. Both types of nanoparticles were dispersed in the resin following the same procedure (sonication-calendaring) and homogenous distribution of the nanoparticles was achieved (Figures 3a and 3c). The fracture mechanism was brittle in the regions free from GNPs and river marks are formed in the resin. The higher brittle area in LY3H25 is indicative that fewer amounts of nanoparticles were incorporated in the matrix (Figure 3c) compared to LY3M25 (Figure 3a).

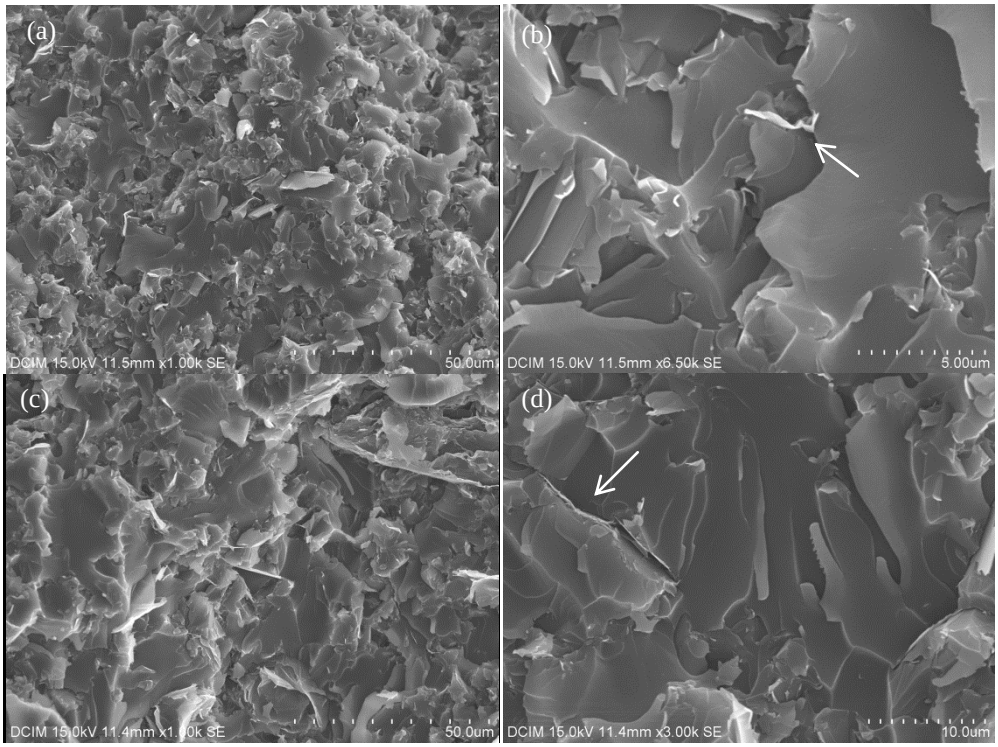

Figure 3. SEM images of fractured surfaces of (a,b) LY3M25 and (c,d) LY3H25 after flexural tests (GNPs are arrowed).

At higher magnification, it was possible to find folded M25 particles while in the case of H25 GNPs they were mainly flat and stacked (Figures 3b and 3d, respectively). On the one hand, M25 folded nanoplatelets have more specific surface but they are folded, so that it is more difficult to form conductive paths. On the other hand, it is difficult to fold stacked H25 GNPs and they keep flat after the dispersion process.

In summary, in the case H25 GNPs the individual particles added into the resin is three times inferior, and combined with the staking phenomenon, the number of nanoparticles dispersed in the matrix is even lower. However, their ability to form conductive networks gives rise to materials with higher electrical conductivity.

3.2. Piezoresistivity of strain sensors

Tensile and flexural tests of both nanocomposites were made, and the variation of electrical resistance was measured simultaneously. The results of structural health monitoring obtained from tensile tests for both nanocomposites are shown in Figure 4. The relative variation of resistance (blue curve in Figure 4) increased as the load also did (black curve in Figure 4). The fracture of these materials was brittle and a sharp jump in the resistance was registered at the end of the test. The shape of the load curves for both nanocomposites was similar. However, the tendency of the resistance curve was different. In the case of LY3M25 the electrical curve was parabolic and for LY3H25 the curve can be fitted to a third order polynomial.

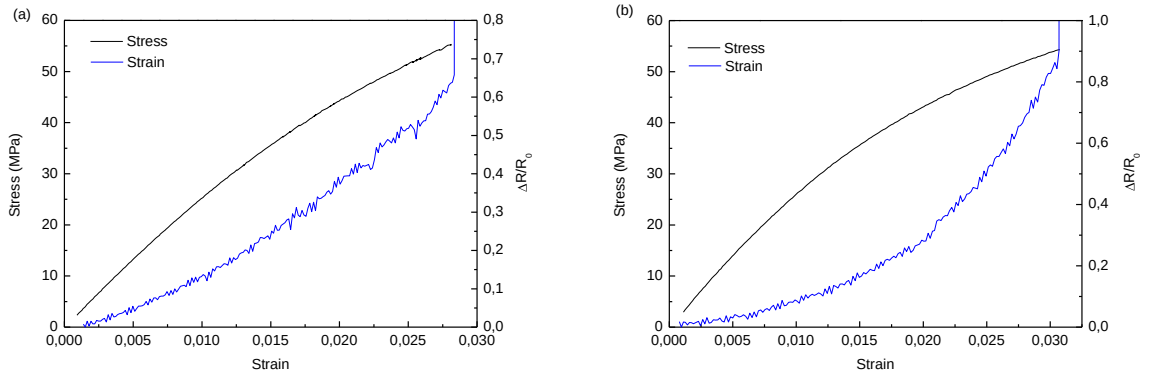

Figure 4. Load-strain and resistance-strain curves of tensile tests of (a) LY3M25 and (b) LY3H25 nanocomposites.

For the case of elastic deformations with strain values lower than 0.005, a linear relationship between resistance and strain can be obtained with a correlation factor, R^2 = 0.999, in both cases. For graphene nanocomposites, preliminary analyses indicate that the piezoresistivity mechanism could be based on tunneling current [10]. The constitutive equation derived by Zhang *et al.* [11] was:

$$R_N = (1+\varepsilon)e^{\gamma s_0 \varepsilon} - 1 \qquad (3)$$

where ε is the deformation, s_0 is the initial tunneling distance (unloaded state) and γ is a factor that depends on the difference in work functions between the graphene conductive filler and the matrix. This equation can be used to model the piezoresistivity of the composite as a function of deformation. In the case of small deformations, the Eq. (3) can be simplified using a Taylor series expansion:

$$R_N \approx (1+\gamma s_0)\varepsilon \qquad (4)$$

This equation explains the initial linear behavior depicted in Figures 4a and 4b, and allows the calculation of the linear gauge factor from the slopes. Using this approach the gauge factor of LY3M25 and LYH25 was 13 ± 1 and 8.7 ± 0.5, respectively. Considering that the traditional metal-foils strain have gauge factors of around 2, with these 3%GNP/epoxy nanocomposites the sensitivity increases up to the order of 6-fold.

At higher deformations, the sensitivity of LY3H25 was larger than that of LY3M25 and reached a value of 30. It could be due to the sparse conductive network formed with H25 nanoplatelets. The small amount of conductive paths made that at higher deformations, their breakage produces large resistance variations. A second phenomenon can be taken place. Kim *et al*. described that at large deformations, the piezoresistivity could be associated to contact resistance between adjacent particles [9]. In the case of graphene nanoplatelets, 2D nanoreinforcements, the piezoresistivity can be influenced by the slippage of nanofillers in the matrix. If the sample is subjected to tensile loads, the contact resistance is increased due to the reduction of the contact area of adjacent or overlaying nanofiller. As it has been explained, the H25 GNPs are stacked and it was possible the nanoplatelets slided ones over each other, increasing the resistance contacts and giving rise to higher sensitivities for this type of nanocomposite sensor. Finally, the GNPs lost the contact and the conductive paths were broken.

The piezoresistivity of LY3M25 and LY3H25 nanocomposites was also measured to characterize the strain response under flexural deformation. Electric contacts were located on tensile and compressive sides of the samples and the strain sensing properties are shown in Figures 5 and 6, respectively. A common characteristic to both nanocomposites is that, at low deformations, the resistance variation was small and decreased with a linear tendency. However from a strain around 0.015, the resistance response changed, increased and became parabolic.

At low strains, $\varepsilon < 0.015$, the sensitivity values were negative for the compression side. It means that compressive states produced the contact between GNPs or tunnel effect and new conductive paths were formed. This phenomenon occurred more significantly in H25 GNPs. In the tensile side, the phenomenon that took place was the opposite and positive values of sensitivity were registered.

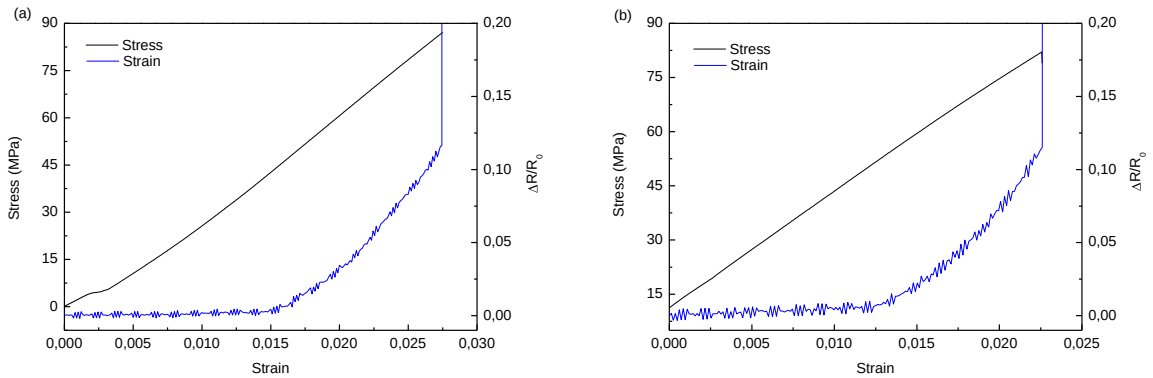

Figure 5. Load-strain and resistance-strain curves in the tensile side of flexural tests of (a) LY3M25 and (b) LY3H25 nanocomposites.

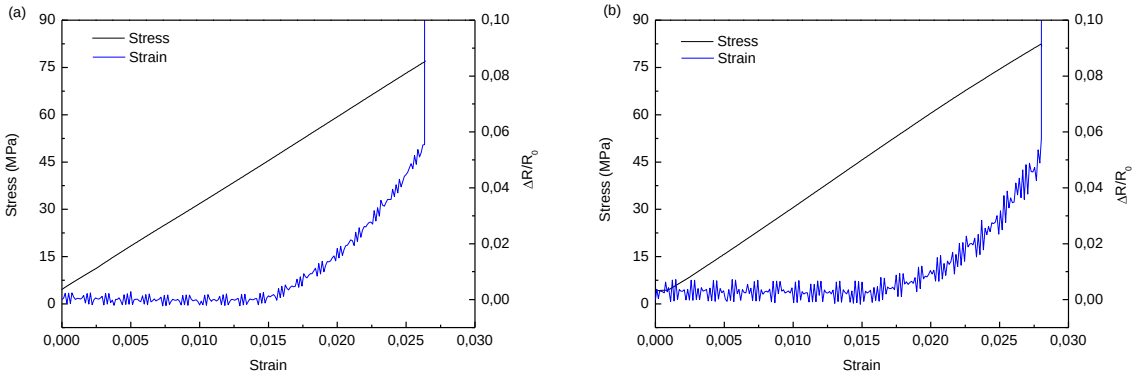

Figure 6. Load-strain and resistance-strain curves in the compression side of flexural tests of (a) LY3M25 and (b) LY3H25 nanocomposites.

At high strains, $\varepsilon > 0.015$, the sensitivity values were positive for compressive and tensile sides. In the tensile surface the predominant phenomenon was the breakage of conductive paths. However, in the compressive surface, apart from the formation of conductive paths, the breakage of them can be taking place. Wang *et al.* reported this phenomenon in the study of carbon nanotube filled silicone rubber composites nanocomposites under compressive loads because the rearranged of the particles in the matrix [5]. Another effect to take into account is that flexural samples had a thickness of 1.7 mm and the electrical contacts registered the resistance response of the whole sample.

The calculated sensitivity values are summarized in Figure 7. In general, the sensitivity values at low deformation range (Figure 7a) were lower than those measured at larger one (Figure 7b) for each load conditions. The maximum gauge factor around 25-30 was measured during the application of uniaxial loads in tensile tests at high deformations. For the case of flexural tests, the larger resistance response was measured in the tensile side, while in the compressive side the sensitivity was an order of magnitude lower. Other authors have obtained gage factors values around 10 for GNPS/epoxy nanocomposites films [9].

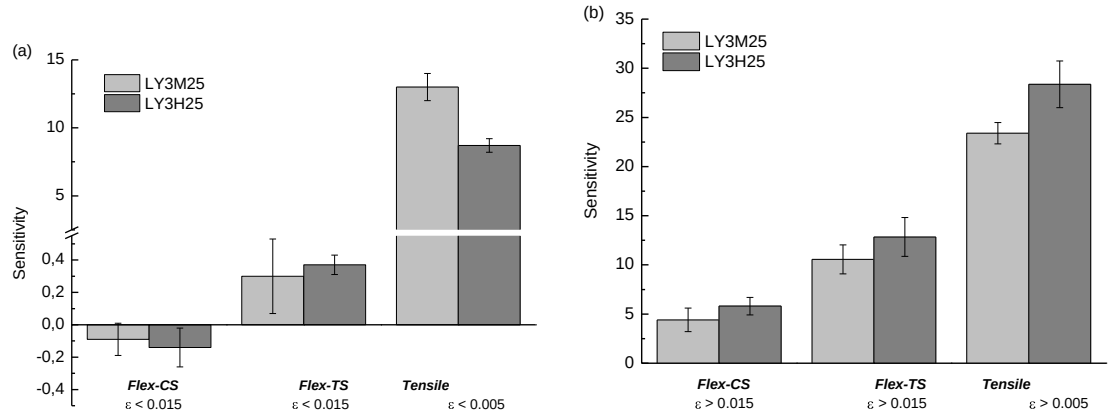

Figure 7. Sensitivity values obtained from flexural and tensile tests at (a) low and (b) high strain values (CS: compression side, TS: Tensile side).

The sensitivity produced by H25 GNPs is in general greater than that given by M25 ones. The results of flexural tests looks like that sensor properties of H25 nanocomposites were better than M25 ones in spite of their bigger testing dispersion. In the case of tensile tests, at high deformations more concluding results were obtained.

Conclusions

We reported GNP/epoxy piezoresistive strain sensors fabricated with two types of nanoplateles with different thickness. This characteristic and the effective number of nanoparticles in the resin had influence on the conductivity and the sensitivity of the sensor. High thickness GNPs involved low amount of nanoparticles added in the resin and keep flat during dispersion. This increased the possibility of conductive paths formation in the material and gave rise to sensors with higher conductivity and sensitivity.

The gauge factors were calculated under tensile and compression loads. At low deformations, the piezoresistance was attributed to changes in tunnel effect and gauge factors around 10 were measured in tensile tests. The higher sensor sensitivities (up to 30 under uniaxial tensile loads) were obtained when the sensors were subjected to high deformations. Variations in the current tunnel, separation between adjacent GNPs or slipping phenomena could be the responsible of the piezoresistance in this range of deformation.

References

[1] J. Robertson. Growth of nanotubes for electronics. *Materials Today*, 10:36-43, 2007.
[2] A.K. Geim and K.S. Novoselov. The rise of graphene. *Nature Materials*, 6:183-191, 2007.
[3] M. H. G. Wichmann, S. T. Buschhorn, J. Gehrmann, and K. Schulte. Piezoresistive response of epoxy composites with carbon nanoparticles under tensile load. *Physical Review B*, 80:245437, 2009.
[4] Ni. Hu, Y. Karube, M. Arai, T. Watanabe, C. Yan, Y. Li, Y. Liu and H. Fukunaga. Investigation on sensitivity of a polymer/carbon nanotube composite strain sensor. *Carbon*, 48(3):680-687, 2010.
[5] Relation between repeated uniaxial compressive pressure and electrical resistance of carbon nanotube filled silicone rubber composite. L. Wang, X. Wang, Y. Li. *Composites Part A: Applied Science and Manufacturing*, 43(2):268-274, 2012.
[6] S. M. Friedrich, A. S. Wu, E.T. Thostenson and T-W. Chou. Damage mode characterization of mechanically fastened composite joints using carbon nanotube networks. *Composites Part A: Applied Science and Manufacturing*, 42(12):2003-2009, 2011.
[7] L. M. Chiacchiarelli, M. Rallini, M. Monti, D. Puglia, J. M. Kenny and L. Torre. The role of irreversible and reversible phenomena in the piezoresistive behavior of graphene epoxy nanocomposites applied to structural health monitoring. *Composites Science and Technology*, 80:73-79, 2013.
[8] S. K. Kumar, M. Castro, A. Saiter, L. Delbreilh, J. F. Feller, S. Thomas and Y. Grohens. Development of poly(isobutylene-co-isoprene)/reduced graphene oxide nanocomposites for barrier, dielectric and sensing applications. *Materials Letters*, 96:109-112, 2013.
[9] Y-J. Kim, J. Y. Cha, H. Ham, H. Huh, D-S. So and I. Kang. Preparation of piezoresistive nano smart hybrid material based on graphene. *Current Applied Physics*, 11(1):S350-S352, 2011.
[10] H. Kim, A. A. Abdala and C. W. MacOsko. *Graphene/polymer nanocomposites*. *Macromolecules*, 43(16):6515-30, 2010.
[11] X-W. Zhang, Y. Pan, Q. Zheng and X-S Yi. Time dependence of piezoresistance for the conductor-filled polymer composites. *Journal of Polymer Science Part B: Polymer Physics*, 38(21):2739-2749, 2000.